

UNCLASSIFIED

Copy  
RM L54L29

NACA RM L54L29

PERSONAL COPY



# RESEARCH MEMORANDUM

AN ANALYSIS OF THE TRANSONIC AND SUPERSONIC PERFORMANCE

LIBRARY COPY

SEVERAL FIXED-GEOMETRY AIR INLETS

FEB 12 1990

By Robert E. Pendley and Robert R. Howell

LANGLEY RESEARCH CENTER  
LIBRARY NACA  
HAMPSHIRE, VIRGINIA

Langley Aeronautical Laboratory  
Langley Field, Va.

LIBRARY COPY

CLASSIFICATION CHANGE

To Unclassified UNCLASSIFIED  
By Authority of RA Date 1/7/55  
Changed by elw

CLASSIFICATION CHANGE

Date 2/90 Declassified

By authority of 123

CLASSIFIED DOCUMENT

This material contains information affecting the National Defense of the United States within the meaning of the espionage laws, Title 18, U.S.C., Secs. 793 and 794, the transmission or revelation of which in any manner to an unauthorized person is prohibited by law.

## NATIONAL ADVISORY COMMITTEE FOR AERONAUTICS

WASHINGTON

March 8, 1955

UNCLASSIFIED

UNCLASSIFIED

NACA RM L54L29



## NATIONAL ADVISORY COMMITTEE FOR AERONAUTICS

## RESEARCH MEMORANDUM

AN ANALYSIS OF THE TRANSONIC AND SUPERSONIC PERFORMANCE  
OF SEVERAL FIXED-GEOMETRY AIR INLETS

By Robert E. Pendley and Robert R. Howell

## SUMMARY

An analysis of the maximum power thrust-minus-drag performance of several turbojet-engine air-inlet combinations was made for a wide range of flight conditions. The principal objective of the analysis was to study by use of experimentally determined drag and total-pressure-recovery characteristics, the range of satisfactory performance of each of several fixed-geometry inlet configurations. Considerations were given to differences of air-flow requirements of various engines. Altitudes ranging from sea level to 35,000 feet and above and flight speeds extending from Mach number of 0 to 2.0 were treated in addition to effects of nonstandard atmospheric temperature. Inlet types considered were the open-nose normal-shock inlet, the wing-root inlet, and the conical-shock inlet.

The results of the analysis showed that, with proper selection of the entrance area, very good performance can be expected of these constant geometry air inlets over a wide range of flight conditions. The extent to which the performance approaches that potentially available with optimum inlet size throughout the Mach number range is shown to be dependent upon the rate at which the engine air flow rises with Mach number and upon the effects of Mach number on the inlet spillage drag variation with mass-flow ratio. It is further shown that an engine of constant corrected weight flow of air tends favorably to maintain a constant inlet-mass-flow ratio at nearly optimum performance but an engine of relatively low rate of air-flow increase with Mach number forces reduced-mass-flow operation upon the inlet as the flight speed is increased; thus, the appearance of performance losses arising from inlet spillage drag results.

Other calculations indicated that the choice of inlet design should favor those of lower minimum drag even though there is associated a greater increase in drag with reduction in mass-flow ratio. An analysis of the effects of ambient temperature on an engine of low rate of air-flow increase with Mach number showed that these effects were as

UNCLASSIFIED

important to the performance of the inlets as those arising from the engine and inlet characteristics.

## INTRODUCTION

Normal-shock fixed-geometry-type inlets have been developed which provide satisfactory performance for turbojet-powered aircraft flying at speeds up to Mach numbers of the order of 1.1. As the flight speed of the aircraft is increased beyond the low supersonic level, the maximum flow rate permitted by the inlet and the flow rate required by the engine diverge and cause the inlet to spill the excess mass of air resulting in spillage drag. In addition, losses in total-pressure recovery increase with Mach number due to the increase in shock loss. The resulting losses in performance have been studied in a number of analyses such as that reported in reference 1. In some such analyses, full theoretical additive drag has been assumed for the spillage drag. In the case of round-lip air inlets, this assumption has been shown by experimental investigations to be invalid. For such inlets, the actual measured spillage drag is in most cases substantially less than the additive drag; hence, the previous performance analyses have overestimated performance losses. In view of the weight and mechanical complexity of any variable-geometry-inlet systems which might be proposed to alleviate these performance losses, it appears worthwhile to reexamine several of the fixed-geometry-inlet systems by using for the performance calculations experimentally determined drag and total pressure-recovery characteristics.

An analysis has, therefore, been made of the influence of several factors on the magnitude of the deviation of the maximum power performance of several fixed-geometry inlets from ideal values. The factors treated were type of inlet, engine-air-flow characteristics, flight altitude, speed, and atmospheric temperature. Inlet types considered were the normal-shock open-nose inlet, the wing-root inlet, and conical-shock inlet, each of which had had its drag and total-pressure-recovery characteristics determined experimentally. These experimentally determined characteristics were used in calculating the performance variations.

## SYMBOLS

A	duct or stream tube cross-sectional area
$C_{De}$	external drag coefficient based on frontal area, $\frac{D_e}{q_o F}$

$C'_{D_e}$	external drag coefficient based on wing area, $\frac{D_e}{q_0 S}$
$D_e$	external drag (additive drag plus pressure and friction drag on external surface)
$F_n$	engine net thrust, $m(V_j - V_o) - (p_j + p_o)A_j$
$\frac{F_n - D_e}{(F_n - D_e)_{\max}}$	performance ratio, the ratio of engine net thrust less external drag for a fixed-geometry inlet to thrust minus drag attainable with inlet of optimum size
$H$	total pressure
$h$	altitude
$M$	Mach number
$m$	inlet or engine mass-flow rate
$m_B$	mass flow of air through area equal to inlet area, for sonic one-dimensional flow with total pressure less than free stream by amount of normal shock loss
$m_c$	mass flow of air at free-stream conditions through area equal to area enclosed by inlet lip (capture area)
$p$	static pressure
$p_A$	atmospheric pressure, NACA standard atmosphere
$T$	total temperature
$t_{\text{std}}$	ambient temperature, NACA standard atmosphere
$W$	engine-air-weight flow rate
$V$	velocity
$\rho$	density
$\delta$	pressure ratio, $\frac{H_2}{(p_A)_{\text{SL}}}$

CONFIDENTIAL

θ temperature ratio,  $\frac{T_2}{(t_{std})_{SL}}$

Subscripts:

o free stream  
1 minimum duct area at inlet  
2 engine compressor inlet  
100 free-stream total pressure at compressor inlet  
j engine exit nozzle station  
max maximum  
SL sea level  
r rated (sea-level static conditions with no total-pressure deficit at compressor inlet)

METHOD OF ANALYSIS

General Approach

The general approach used in the analysis consisted of fixing the inlet area at a value which would induct the full engine air-flow requirement at  $M_0 = 0.9$  and at an altitude of 35,000 feet in an NACA standard atmosphere. The inlet size was then held constant at this value and the maximum-power thrust-minus-drag performance of the engine-inlet system was then compared over a broad range of flight conditions with the maximum available upon use of the optimum inlet size. The analysis thus required the calculation of the performance of the inlet with various inlet entrance-duct areas. Since the maximum outer dimension of the body housing the engine is normally fixed by other than inlet considerations, the inlet-area variations result in variations of the external and internal lines from the inlet lip rearward. An exact analysis would thus require drag and pressure-recovery data for a very large number of internal and external shapes which, of course, are not available. Fortunately, however, the extent of the inlet-area variation included in the analysis was not so great as to involve large changes in the inlet diameter (or lip height and width) relative to the distance between the inlet lip and that point downstream which is unaffected by changes in inlet size. The drag data of reference 2 indicate that, when

the larger values of inlet-lip fineness ratio (corresponding to low drag) are considered, only small changes in external drag are to be expected with substantial changes in inlet size for a fixed inlet length. Reference 3 similarly indicates a negligible effect on the pressure recovery may be expected of the internal geometry changes involved in the analysis. For each type of inlet considered, drag and pressure-recovery data for an inlet of fixed specific proportions was necessarily used but, for the reasons indicated above, their use in the analysis is considered acceptable.

#### Basic Data

Experimental drag data for the configurations shown in figure 1 (refs. 4 to 6) were supplemented in the calculations by spillage drag data from references 3 and 7. The forebody of inlet I was an NACA 1-49-300 nose inlet, and inlet V was identical with inlet I forward of a station just downstream of the inlet lip; downstream from this station, a conical profile of  $4.4^\circ$  half-angle replaced the fuller 1-series profile. The central body of the conical-shock inlet had a  $25^\circ$  half-angle and the lip position parameter was  $46^\circ$ . Since transonic and supersonic inlet data have been obtained almost exclusively for research configurations, an exact analysis of the performance of the internal-flow system as installed in a complete aircraft is not possible. The drag coefficients used in this analysis are those as measured for the research configurations. Although the method of presentation and comparison of the results was selected so as to tend to circumvent this limitation, this fact should be remembered in interpreting the quantitative significance of the results.

The engine thrust characteristics used in the analysis are shown in figure 2. The assumed sea-level rated thrust without afterburner was 8,700 pounds at a rated air flow of 15.8 pounds per second per square foot of frontal area. These curves were assumed as the thrust variation of engines of differing air-flow characteristics to be discussed below. Disregarding in this manner such association as exists between air-flow and thrust variation with flight speed is considered acceptable for the purpose of this analysis because of the ratio form of thrust-minus-drag calculation.

The manner in which the engine air flow rises with flight Mach number is of primary importance in establishing the performance of a fixed-geometry system. Substantial differences exist in this characteristic among various engines, as is illustrated by the curves for three different engines (engines 1, 2, and 3) in figure 3. An engine of constant corrected weight flow  $\frac{W\sqrt{\theta}}{S}$  would have an air-flow curve (designated as  $S/\sqrt{\theta}$ ) which rises more rapidly with Mach number than that of any of the

three conventional engines shown. The curves for the constant corrected weight-flow engine and for engine 3 are assumed for the present analysis to represent limits between which most turbojet engine characteristics will fall and the air-flow characteristics of these two engines were therefore used in the analysis.

As is shown in figure 4, spillage drag characteristics vary widely for different inlets. Except for the test point at the highest Mach number of the sweptback-wing-root-inlet test, the theoretical spillage drag curve from reference 8 indicates rather well the trends of spillage drag with Mach number. In all cases, the external drag coefficient is based on the same area relative to the inlet area. Although inlets I and V had identical lip shapes, the drag-curve slopes were substantially different at transonic and supersonic speeds. The curves faired arbitrarily through the test points for the round-lip nose inlets were used in the analysis and are thought to represent possible extremes of drag-curve slopes for such inlets. The additive-drag-curve slope was used in addition to the experimental drag-curve slope in a portion of the analysis to show the effect of maximum spillage drag on performance.

Drag and pressure-recovery characteristics used in the calculations for the open-nose inlets I and V appear in figures 5 to 7. The drag curves for  $m/m_0 = 1.0$  (fig. 5) were obtained in free-flight measurements on fin-stabilized research bodies and for the drag curves against mass-flow ratio (fig. 6) were constructed from those of figures 4 and 5. Inasmuch as the geometric proportions, afterbodies, and fins were identical for inlets I, V, and the conical shock inlet (fig. 1), a direct comparison of external drag can be made. Data obtained in the tests reported in references 3 and 9 were used in preparing the normal-shock nose-inlet pressure-recovery data (fig. 7). It is assumed in the analysis that the pressure-recovery characteristics are independent of external shape.

Data obtained with the wing-root inlet configuration of reference 5 and hitherto unpublished were used in the analysis and are presented in figure 8. In the preparation of the conical-shock inlet curves of figure 9, external drag values at maximum mass-flow ratios were obtained from reference 6, spillage drag data from reference 7, and pressure-recovery data from reference 10.

#### Procedure

When referenced to a specific engine, a given area of the inlet will correspond to a mass-flow ratio at which the inlet will deliver a certain pressure recovery to the engine and a certain drag contribution to the external flow. The engine thrust minus the external drag can thus be calculated as a function of mass-flow ratio and typical results

~~CONFIDENTIAL~~

of such a calculation are given for the nose inlets I and V in figure 10. As the flight speed is increased beyond Mach number 1.0, the external-drag-curve slope increases, and the peak performance of the system tends to occur at mass-flow ratios near, but somewhat less than, the choking values.

After the calculation of the curves illustrated in figure 10, a first trial selection of the inlet areas was made. Since operation of the inlets in the oversized condition was anticipated at the higher flight speeds, the areas were chosen to correspond to  $m/m_s = 0.94$  at  $M_0 = 0.9$ ; this condition was deemed as close an approach to choking conditions as would be desirable (see fig. 7). At other Mach numbers the inlet operates at mass-flow ratios which are determined by the engine air-flow characteristics. The matched mass-flow ratio at each Mach number was determined from the intersection of two curves of mass flow against mass-flow ratio; one of the curves represents the allowable mass flow through the inlet,  $(\dot{m} = (m/m_s)\rho_s V_s A_1)$ , and the other curve represents the mass required by the engine for the total-pressure conditions at the compressor inlet,  $(\dot{m} = H_2/H_0(m_{100}))$ . The resulting mass-flow ratio schedules for engines 8/ $\sqrt{6}$  and 3 operating with the pressure-recovery characteristics of figure 7 are shown in figure 11. Since the mass-flow ratios imposed by the engines are thus known, per-

formance ratios  $\frac{F_n - D_e}{(F_n - D_e)_{\max}}$  of the matched systems may then be read

from the curves of figure 10 and are indicated on these curves by ticks at the appropriate mass-flow ratios. After an examination of the performance with the first trial inlet size, improved compromises were achieved, as will be discussed later with other choices of inlet area.

## DISCUSSION OF RESULTS

### Performance at 35,000 Feet

The performance in an NACA standard atmosphere of the fixed-geometry systems treated are presented in figures 12 and 13 in terms of the optimum thrust minus drag available to the particular inlets considered at each Mach number. As stated in the previous section, a first trial inlet area was calculated for each inlet-engine combination to correspond to  $m/m_s = 0.94$  at  $M_0 = 0.9$ , the results of which are indicated in figures 12 and 13 (together with those for other sized inlets in figure 12).



For all inlets, (figs. 12 and 13) the  $8/\sqrt{6}$  engine tended to keep the inlet mass flow at an approximately constant fraction of the maximum possible (figs. 11 and 13), and the thrust-minus-drag ratios for inlets combined with this engine did not vary greatly with Mach number. All design mass-flow ratios and corresponding inlet areas considered are tabulated in table I.

The air-flow characteristics of engine 3 were such as to impose a continuously diminishing mass-flow ratio on the systems as the Mach number was increased. The performance curves thus became influenced by inlet spillage drag and pressure-recovery variation with mass-flow ratio. Inlet I, which had the least drag-curve slope, performed well throughout the Mach number range in spite of the low mass-flow ratio imposed by engine 3 at higher Mach numbers. Even with the relatively high drag curve slope of inlet V, the performance deficit was only 6 percent at the highest Mach number when combined with this engine; it is thus indicated that excessive performance losses need not be expected of fixed-geometry normal-shock nose inlets at Mach numbers up to 1.5 when subject to engine air-flow characteristics varying between those of the two engines considered.

An examination of figure 10 will disclose that a value of design mass-flow ratio for inlet I with the  $8/\sqrt{6}$  engine lower than the value of 0.94 picked initially would have constituted a more favorable selection. Sizing the inlet in this case for a design mass-flow ratio of 0.90 at  $M_0 = 0.9$  resulted in optimum or very close to optimum performance over the entire Mach number range (fig. 12(a)). A substantially better choice of area was made for the wing-root inlet also; the performance was optimum or within 1/2 percent of optimum at all Mach numbers treated with an inlet of design mass-flow ratio 0.80 (fig. 12(c)).

The initial choice of design mass ratio proved to be reasonably satisfactory for the wing-root inlet with engine 3. Calculations were made for an increased area of this inlet (design mass flow ratio 0.84) with the purpose of obtaining improved performance at the design speed. The results show that the improvement attained was made at a great sacrifice in performance at the higher speeds, where the lowered mass-flow ratios imposed by engine 3 caused losses in the form of spillage drag and even more important losses in thrust because of the reduced total-pressure recovery. The latter difficulty arises from the characteristic tendency of the fuselage side air inlet toward lowered pressure recoveries at reduced mass-flow ratios because of losses due to entrainment of the fuselage boundary layer.

The effect of the air-flow characteristics of engine 3 on the conical shock inlet was to force such a low-mass-flow-ratio condition on the system at the higher speeds as to result in intolerable performance losses and probably internal flow instability (fig. 13). As has been

indicated in a number of previous other works, the necessity of some form of inlet area control is clear for engines of such air-flow characteristics at Mach number of 1.5 and above.

### Inlet Design Considerations

The foregoing analysis indicates the extent to which a fixed-geometry inlet of a particular design can approach the maximum performance available to that same type of inlet configuration with the entrance area adjusted to the optimum value. When the design of a complete aircraft configuration is under analysis, and the inlet design has been established in general form, the external lines of the internal-flow system can be efficiently combined with those of the other aircraft components in such a manner as to arrive at a cross-sectional area distribution like that of a low-drag body of revolution (ref. 11). The drag of the airplane is thus controlled largely by the smoothness and equivalent fineness ratio of the cross-sectional area diagram of the entire configuration rather than by summation of the drag contribution of isolated components such as air inlets. Upon attaining a satisfactory overall area diagram, the designer's interest in the isolated drag contribution of the air inlets will be of a secondary nature. If the performance of a fixed-geometry inlet system is then appraised, the propul-

sive thrust ratio  $\frac{F_n - D_e}{(F_n - D_e)_{\max}}$  as calculated for the configuration

under consideration will indicate clearly the worth of each inlet size considered.

In those cases where it is desired to appraise the performance of isolated ducted bodies, the quantity  $\frac{F_n - D_e}{(F_n - D_e)_{\max}}$ , which, as stated

before, expresses the proximity of the performance of a particular system to its peak performance, indicates only the inlet size required for the best compromised performance. Although an inlet may be shown to operate favorably close to its optimum performance in this manner, the designer must further consider whether the optimum performance itself is good and, in cases where a choice in inlet type is available, must compare the performance of the different designs considered in an absolute sense.

In figure 12, for example, it was shown that the low drag-curve slope of inlet I permitted the system to operate more closely to optimum conditions than did inlet V. Although the drag-curve slope of inlet V is the less favorable, it is known that, above a Mach number of approximately 1.1, its drag at maximum mass-flow ratios is lower than that of inlet I (fig. 5). Under the reduced-mass-flow-ratio conditions

associated with supersonic operation of the inlets as designed for  $M = 0.9$ , the question as to whether the spillage drag of inlet V will be as large as to result in supersonic thrust minus drag performance inferior to that of inlet I must be considered. The propulsive thrust was therefore calculated as a fraction of engine ideal thrust in figure 14 for inlets I and V. Figure 14(a) was calculated for the engine of constant corrected mass flow and since the mass-flow ratios for this engine remain at a high, nearly constant value, spillage drag does not enter materially in the performance, which, therefore, reflects the drag advantages of inlet V at high mass-flow ratios.

The reduced-mass-flow ratios imposed at supersonic Mach numbers by engine 3 result in greater spillage drag for inlet V, but figure 14(b) shows nevertheless that the initial drag advantage of inlet V at high-mass-flow ratios is sufficiently great to result in higher values of propulsive thrust at supersonic Mach numbers. Hence, it is indicated that, for the range of engine air flow and free-stream Mach numbers considered, it would be desirable to favor a low minimum drag inlet configuration rather than one with a low drag-curve slope. This is thought to be generally true since the crossover point of the curves for drag against mass-flow ratio for the various open-nose inlets of reference 4 occurs outside the most efficient inlet-engine operating range of the present analysis. It appears, therefore, that a choice of open-nose inlet design, subject only to aerodynamic evaluation, should probably depend primarily on the minimum drag characteristics of the inlet body and not on the drag-curve slope. A method for obtaining practical minimum-drag nose-inlet bodies is presented in reference 12.

#### Speed Range of Efficient Normal-Shock Inlet Performance

The uniformity of the fins and afterbodies of the inlet configurations of references 4 and 6 makes possible a performance comparison which indicates the Mach number region in which the normal-shock inlet must be abandoned in favor of the higher pressure recoveries obtainable with the use of external supersonic compression. Calculations for the engine of constant corrected weight flow were made with this purpose in mind, and the results are shown in figure 15. Experimental data for normal-shock inlets at Mach numbers in excess of 1.5 are unavailable. The drag at these higher Mach numbers was therefore estimated as indicated by the dashed portion of the curve for inlet V (fig. 5) and the pressure recovery was estimated by reducing the  $M_0 = 1.0$  curve (fig. 7) by the appropriate normal-shock total-pressure loss.

The usefulness of the normal-shock inlet appears to terminate at flight speeds between  $M_0 = 1.5$  and  $M_0 = 1.6$ . At higher speeds, the pressure-recovery inferiority of the normal-shock inlet results in a continuously increasing loss in performance relative to that of the

CONFIDENTIAL

conical-shock inlet. At lower speeds, the performance of the normal-shock inlet is probably unexcelled.

#### Effect of Altitude on Performance of the Fixed-Geometry System

Except for the effects of Reynolds number, the corrected weight flow of air to a turbojet engine at a given Mach number and revolution per minute is independent of altitude above approximately 35,000 feet. The system-mass-flow-ratio variation with Mach number will, therefore, remain constant and performance curves of figures 12 and 13 will hold at altitudes above 35,000 feet. The inlets as designed for  $M_0 = 0.9$ ,  $m/m_s = 0.94$ , and an altitude of 35,000 feet would be forced by the engine air flow to operate at the following mass-flow ratios at the sea-level static condition if there were no total-pressure deficit at the compressor inlet:

Inlet	Engine	$A_1$	$\frac{m_{100}}{m_s}$
I and V	3	3.42	0.857
I and V	$8/\sqrt{6}$	3.04	.966
Wing root	3	3.34	.882
Wing root	$8/\sqrt{6}$	2.96	.998
Conical shock	3	3.38	.868
Conical shock	$8/\sqrt{6}$	3.01	.976

Actually, of course, total-pressure losses will appear at the compressor inlet and the actual mass-flow ratios at static sea-level conditions will be favorably less than these tabulated values being reduced in direct proportion to the total pressure at the compressor inlet. The air-flow demands on all inlets considered above will, therefore, be less than the amount which the inlet could deliver with isentropic flow and Mach number unity at the inlet minimum area. The actual choking mass-flow ratio of an inlet at static conditions is a sensitive function of the inlet lip design (see refs. 13 and 14); and the duct surface immediately adjacent. Among the inlets considered, the conical-shock inlet is the most vulnerable to choking and large total-pressure losses at the static condition because of its sharp lip.

At a Mach number of 0.9 at sea level, which represents entry of the climb condition, inlet-engine combinations which showed good performance in figure 12 also will operate at satisfactory mass-flow ratios:

CONFIDENTIAL

Inlet	Engine	$\frac{m}{m_s}$	$\frac{F_n - D_e}{(F_n - D_e)_{\max}}$
I and V	3	0.68	1.00
I and V	$8/\sqrt{6}$	.94	.98
Wing root	3	.68	1.00
Wing root	$8/\sqrt{6}$	.82	.99

The propulsive thrust ratio was not evaluated for the conical-shock inlet for the lack of drag and pressure-recovery data, but operation at satisfactory mass-flow ratios may be expected because of the similarity of its inlet area and that of the nose inlets.

One may infer from the foregoing calculations that the method used to select the inlet area in this analysis will provide a fixed-geometry inlet of satisfactory performance at sea-level take-off and climb conditions and at high-speed conditions at and above 35,000 feet, except in those cases where engines of relatively low air-flow increase with Mach number are to be operated at flight Mach numbers above 1.5.

#### Effect of Nonstandard Air on the Performance of a Fixed-Geometry System

The analysis has so far treated the case of engine-inlet performance in the NACA standard atmosphere. The engine air-flow characteristics are materially affected by the atmospheric temperature, however, and the performance on a hot (standard temperature +40° F) and a cold (standard temperature -40° F) day was therefore calculated for the inlets as designed for  $M_0 = 0.9$  at 35,000 feet in a standard atmosphere. (Note that the effect of ambient temperature on the absolute performance does not appear in these calculations.) As shown in figure 16, engine 3 requires higher mass-flow ratios on the cold day and lower mass-flow ratios on the hot day. For any specified Mach number, the mass-flow ratio of the inlet with the engine of constant weight flow ( $8/\sqrt{6}$ ) will remain independent of altitude and atmospheric temperature, if the effects on the diffuser pressure recovery of the concomitant variation in Reynolds number are neglected.

Standard-atmosphere performance curves of figure 12 are reproduced in figure 17 for comparison with the points calculated for the hot and cold day. The propulsive thrust ratios for the nonstandard conditions express the propulsive thrust realized under these conditions as a fraction of the propulsive thrust possible with the optimum inlet size under those same conditions. The points were calculated for flight at true airspeeds corresponding to  $M = 0.9, 1.2$ , and  $1.5$  in the standard atmosphere. The temperature effects on the fraction of the performance

potential realized is greater than the effects originating in the characteristics of the engine air flow. The mass-flow ratios on the cold day are so high as to be marginal with respect to choking (fig. 16) at the lower Mach numbers and the performance is reduced there because of reduced pressure recovery. Performance gains result at the higher Mach numbers where the increased mass-flow ratio reduces the spillage drag. Converse effects were obtained for the hot day; that is, performance losses due to spillage drag are increased at the higher Mach numbers and at the lower Mach numbers the drag-curve slopes are low enough to permit a net gain in performance as a result of pressure-recovery improvement.

The inlet with engine 3 will operate at the following mass-flow ratios with no total-pressure losses at the sea-level static condition:

Temperature	$(m/m_s)_{100}$
$t_{std} - 40^\circ F$	0.954
$t_{std}$	.857
$t_{std} + 40^\circ F$	.764

As may be inferred from the tests of reference 14, inlets of sufficiently rounded lips will be free of choking under the above conditions since for the case of highest mass-flow ratio (cold day) a pressure recovery as high as 0.95 will result in a mass-flow ratio of approximately 0.90.

#### SUMMARY OF RESULTS

The extent to which the performance of a fixed-area inlet approaches that potentially available with an inlet of constantly variable size throughout the Mach number range is dependent upon the rate at which the engine air flow rises with Mach number and upon the effects of Mach number on the inlet spillage drag variation with mass-flow ratio. In the present analysis, several specific normal-shock inlets were studied over a Mach number range up to 1.5 and a conical-shock inlet was studied up to Mach number of 2.0 by using experimentally determined drag and pressure-recovery data. It was shown that fixed-area versions of all the inlets considered can operate at nearly optimum performance at take-off, climb, and high-speed high-altitude flight at Mach numbers extending at least to the limits of the analysis when matched with an engine of constant corrected weight flow. With an engine of relatively low rate of air-flow increase with Mach number, approximately optimum performance also can be realized with an inlet of low spillage drag rate at Mach numbers extending

up to at least 1.5 whereas an inlet of high spillage drag rate provides a somewhat lower performance as a result of operation at lowered mass-flow ratios. In the case of the latter engine, the mass-flow ratios at Mach numbers from 1.5 to 2.0 are so low as to result in great performance losses and possible inlet instability for a conical shock inlet; in which case some form of variable geometry is apparently necessary.

Other considerations indicate that the choice of inlet design should favor those of low minimum drag even though there be associated a greater increase in drag with reduction in mass-flow ratios. It was also shown that the performance of the conical-shock inlet considered exceeded that of the normal-shock open-nose inlets at a Mach number between 1.5 and 1.6.

The performance of inlets matched with an engine of constant corrected weight flow was shown to be relatively independent of ambient temperature. For the engine of low rate of air flow, the effects of ambient temperature were found to be as important to the inlet performance as engine characteristic or inlet design, with the possibility of inlet choking at the lower flight speeds on a cold day.

Langley Aeronautical Laboratory,  
National Advisory Committee for Aeronautics,  
Langley Field, Va., December 13, 1954.

## REFERENCES

1. Schueller, Carl F., and Esenwein, Fred T.: Analytical and Experimental Investigation of Inlet-Engine Matching for Turbojet-Powered Aircraft at Mach Numbers Up to 2.0. NACA RM E51K20, 1952.
2. Pendley, Robert E., Milillo, Joseph R., Fleming, Frank F., and Bryan, Carroll R.: An Experimental Study of Five Annular-Air-Inlet Configurations at Subsonic and Transonic Speeds. NACA RM L53F18a, 1953.
3. Pendley, Robert E., Milillo, Joseph R., and Fleming, Frank F.: An Investigation of Three NACA 1-Series Nose Inlets at Subsonic and Transonic Speeds. NACA RM L52J23, 1953.
4. Sears, R. I., Merlet, C. F., and Putland, L. W.: Flight Determination of Drag of Normal-Shock Nose Inlets With Various Cowling Profiles at Mach Numbers From 0.9 to 1.5. NACA RM L53I25a, 1953.
5. Howell, Robert R., and Trescot, Charles D., Jr.: Investigation at Transonic Speeds of Aerodynamic Characteristics of a Semielliptical Air Inlet in the Root of a 45° Sweptback Wing. NACA RM L53J22a, 1953.
6. Merlet, Charles F., and Putland, Leonard W.: Flight Determination of the Drag of Conical-Shock Nose Inlets With Various Cowling Shapes and Axial Positions of the Center Body at Mach Numbers From 0.8 to 2.0. NACA RM L54G21a, 1954.
7. Weinstein, Maynard I., and Davids, Joseph: Force and Pressure Characteristics for a Series of Nose Inlets at Mach Numbers From 1.59 to 1.99. III - Conical-Spike All-External-Compression Inlet With Supersonic Cowl Lip. NACA RM E50J30, 1951.
8. Fraenkel, L. E.: The External Drag of Some Pitot-Type Intakes at Supersonic Speeds. Part I. Rep. No. Aero. 2380, British R.A.E., June 1950.
9. Sears, Richard I., and Merlet, C. F.: Flight Determination of Drag and Pressure Recovery of a Nose Inlet of Parabolic Profile at Mach Numbers From 0.8 to 1.7. NACA RM L51E02, 1951.
10. Allen, J. L., and Beke, Andrew: Force and Pressure Recovery Characteristics at Supersonic Speeds of a Conical Spike Inlet With Bypasses Discharging in an Axial Direction. NACA RM E52K14, 1953.
11. Whitcomb, Richard T.: Recent Results Pertaining to the Application of the "Area Rule." NACA RM L53I15a, 1953.

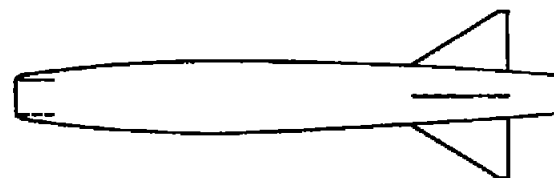


12. Howell, Robert R.: A Method for Designing Low-Drag Nose-Inlet-Body Combinations for Operation at Moderate Supersonic Speeds. NACA RM L54IO1a, 1954.
13. Bryan, Carroll R., and Fleming, Frank F.: Some Internal-Flow Characteristics of Several Axisymmetrical NACA 1-Series Nose Air Inlets at Zero Flight Speed. NACA RM L54EI9a, 1954.
14. Milillo, Joseph R.: Some Internal-Flow Characteristics at Zero Flight Speed of an Annular Supersonic Inlet and an Open-Nose Inlet With Sharp and Rounded Lips. NACA RM L54EI9, 1954.

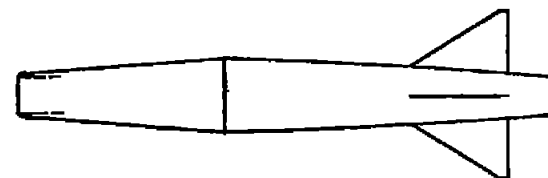
TABLE I.- DESIGN MASS-FLOW RATIOS AND CORRESPONDING INLET AREAS

Inlet	Engine	Design <sup>1</sup> $\frac{m}{m_s}$	A <sub>1</sub> , sq ft
I	$\delta/\sqrt{\theta}$	0.94	3.04
	3	.94	3.42
V	$\delta/\sqrt{\theta}$	.94	3.04
	3	.94	3.42
Wing root	$\delta/\sqrt{\theta}$	.94	2.96
	3	.94	3.34
Conical shock	$\delta/\sqrt{\theta}$	.94	3.01
	3	.94	3.38
Resized inlet I	$\delta/\sqrt{\theta}$	.90	3.20
Resized wing root inlet	$\delta/\sqrt{\theta}$	.80	3.48
	3	.84	3.80

<sup>1</sup>At design  $M_0 = 0.90$ .



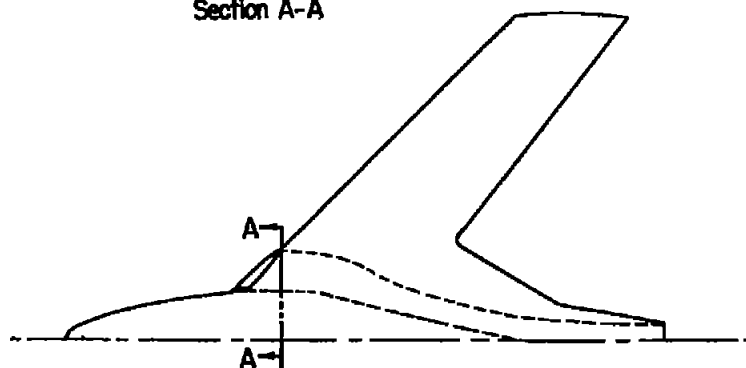
Inlet I (ref. 4)



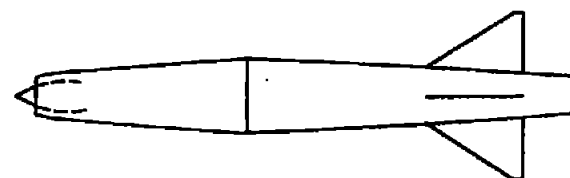
Inlet V (ref. 4)



Section A-A



Wing-root Inlet (ref. 5)



Conical-shock Inlet (ref. 6)

Figure 1.- Sources of drag data for the inlets considered.

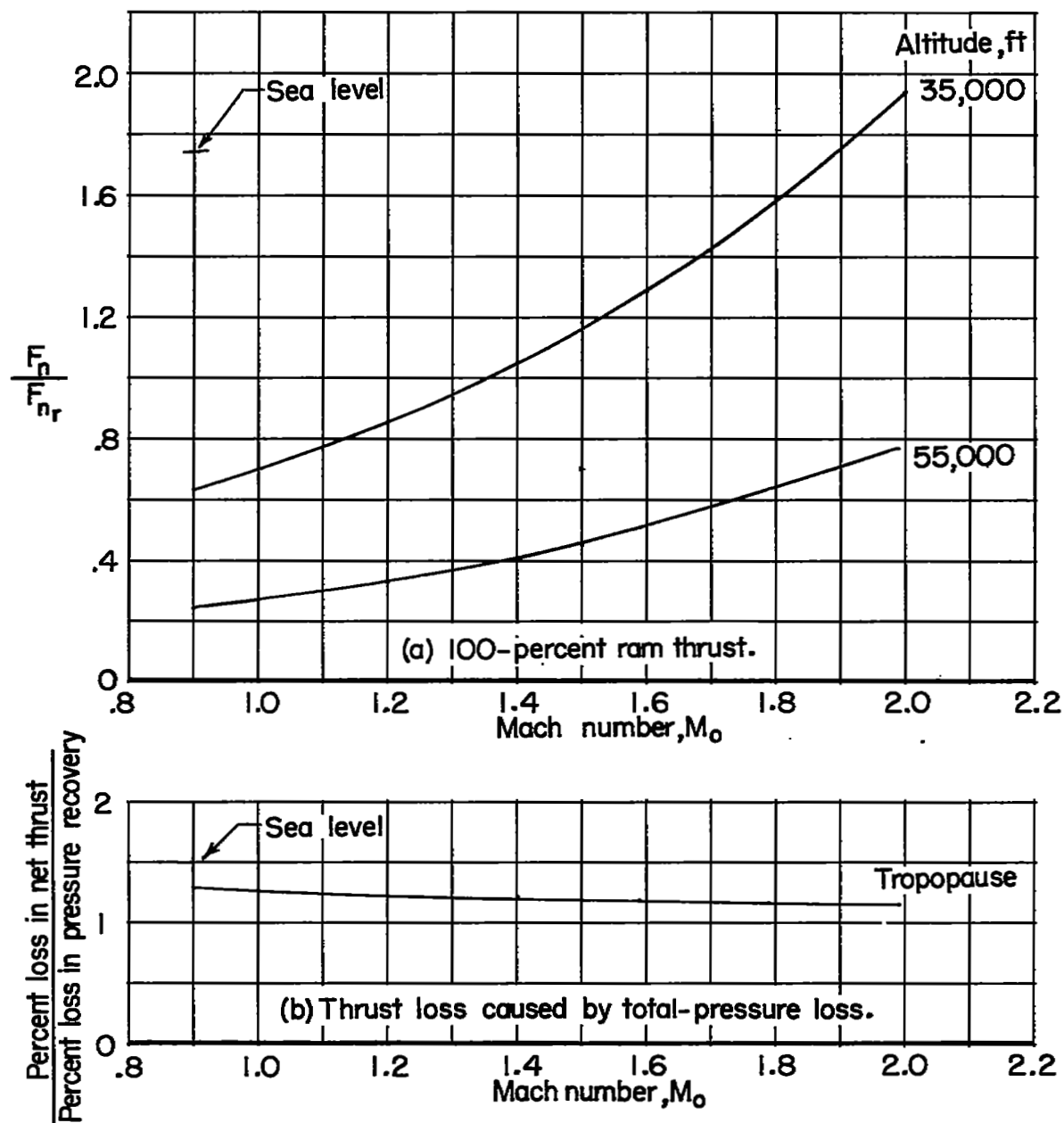


Figure 2.- Assumed net thrust characteristics, full afterburning.

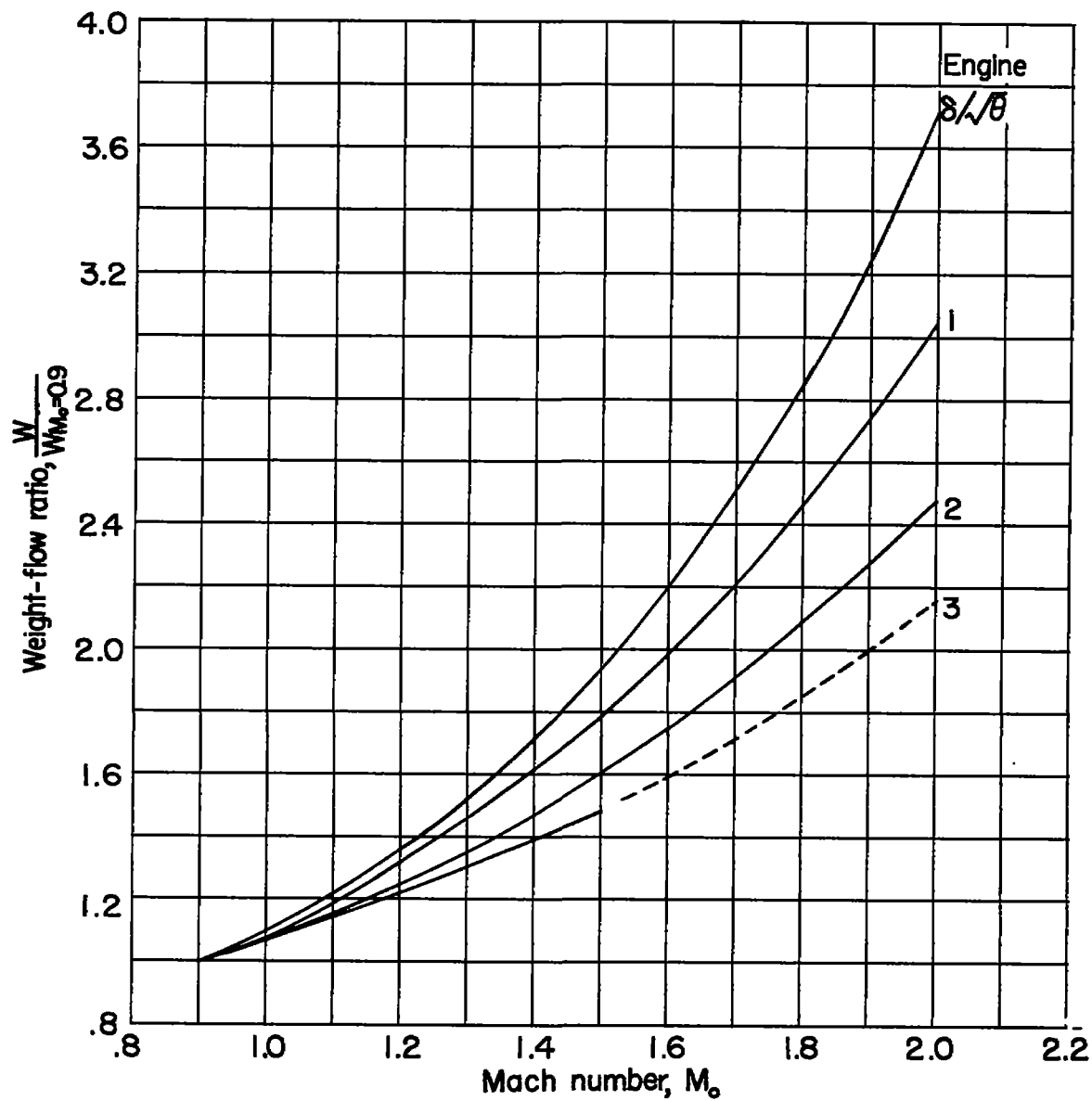


Figure 3.- Engine air-flow characteristics.

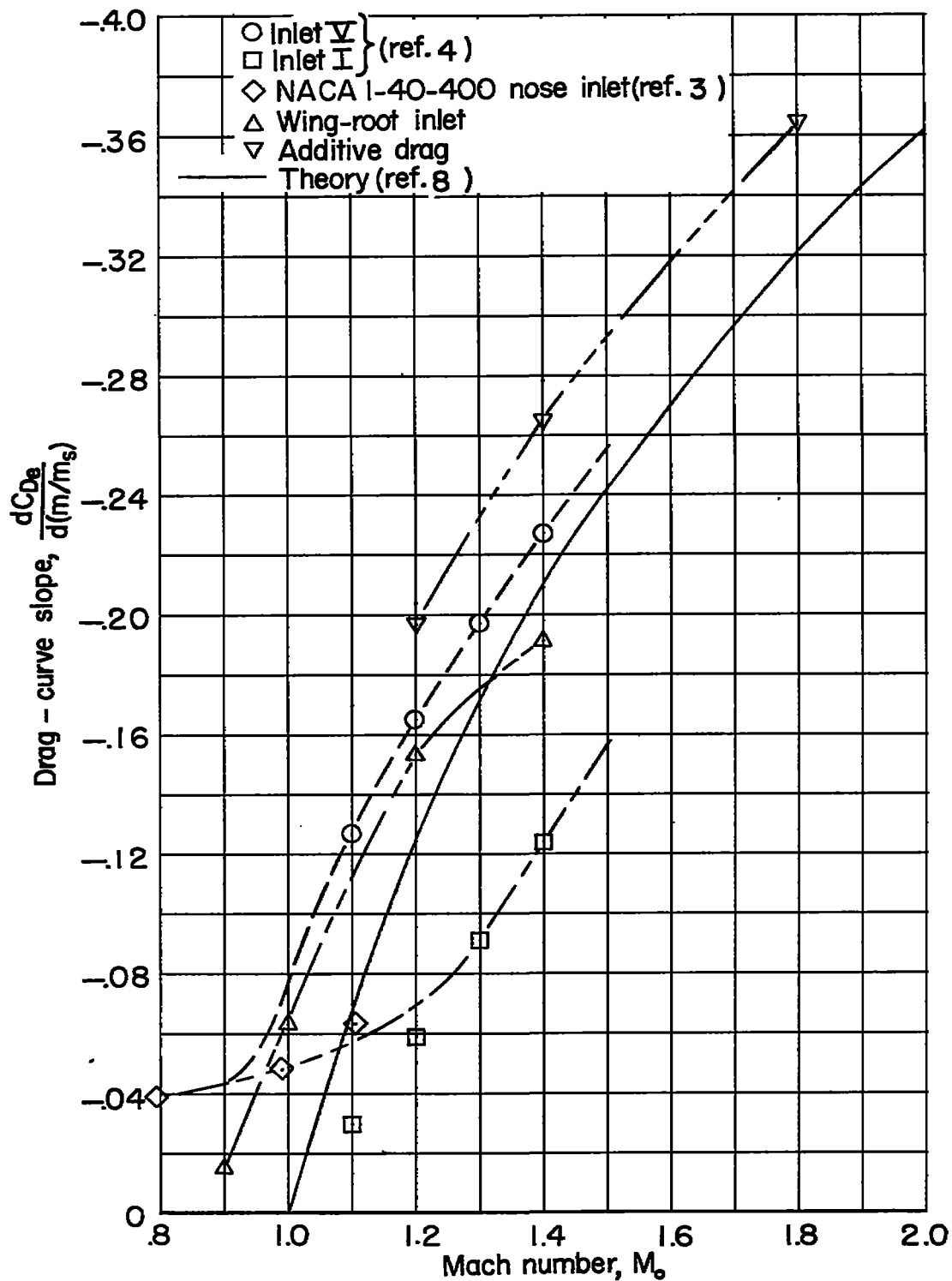


Figure 4.- Variation of drag-curve slope with Mach numbers.

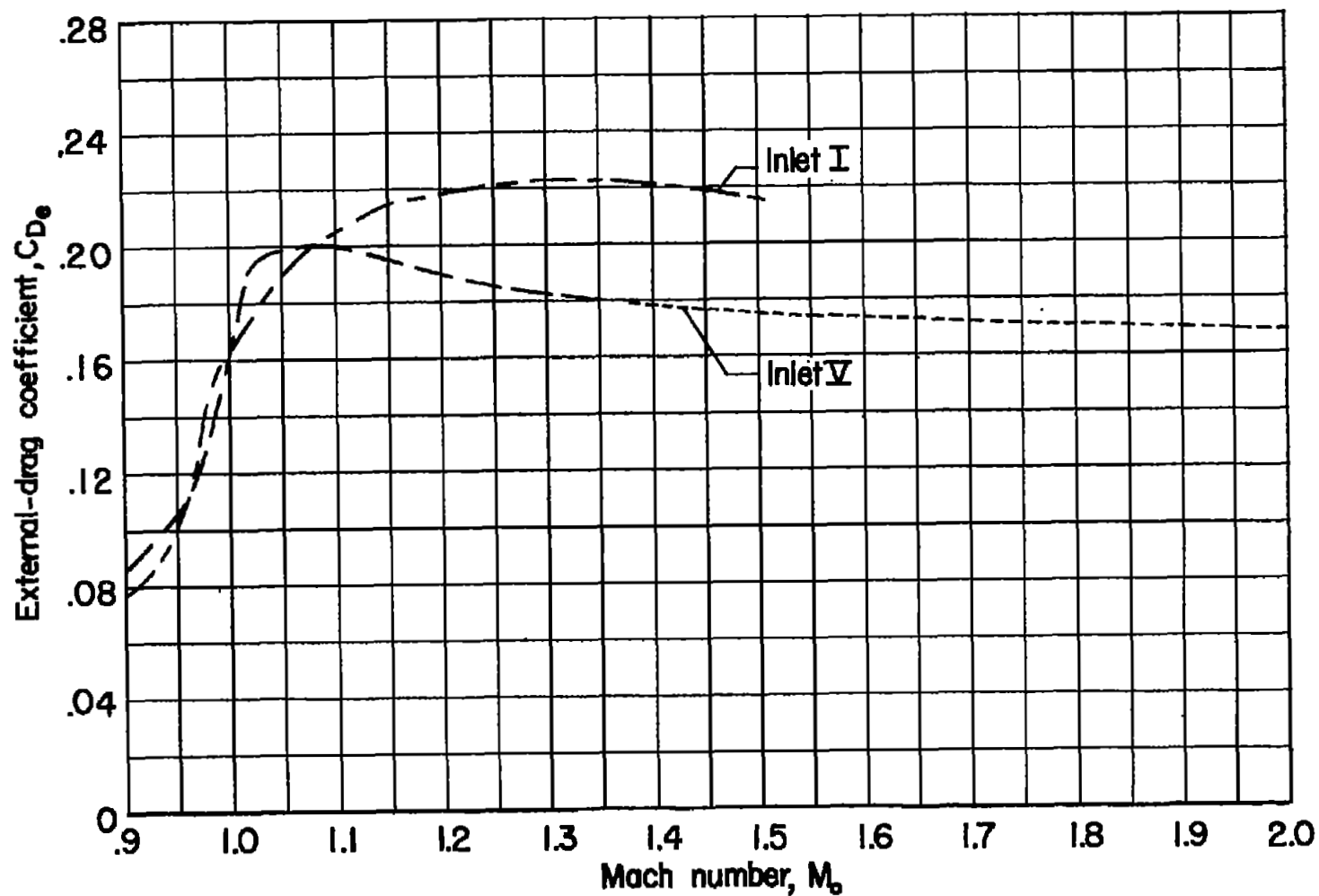


Figure 5.- External-drag curves for two of the configurations of reference 4.  $\frac{m}{m_o} = 1.0$ .

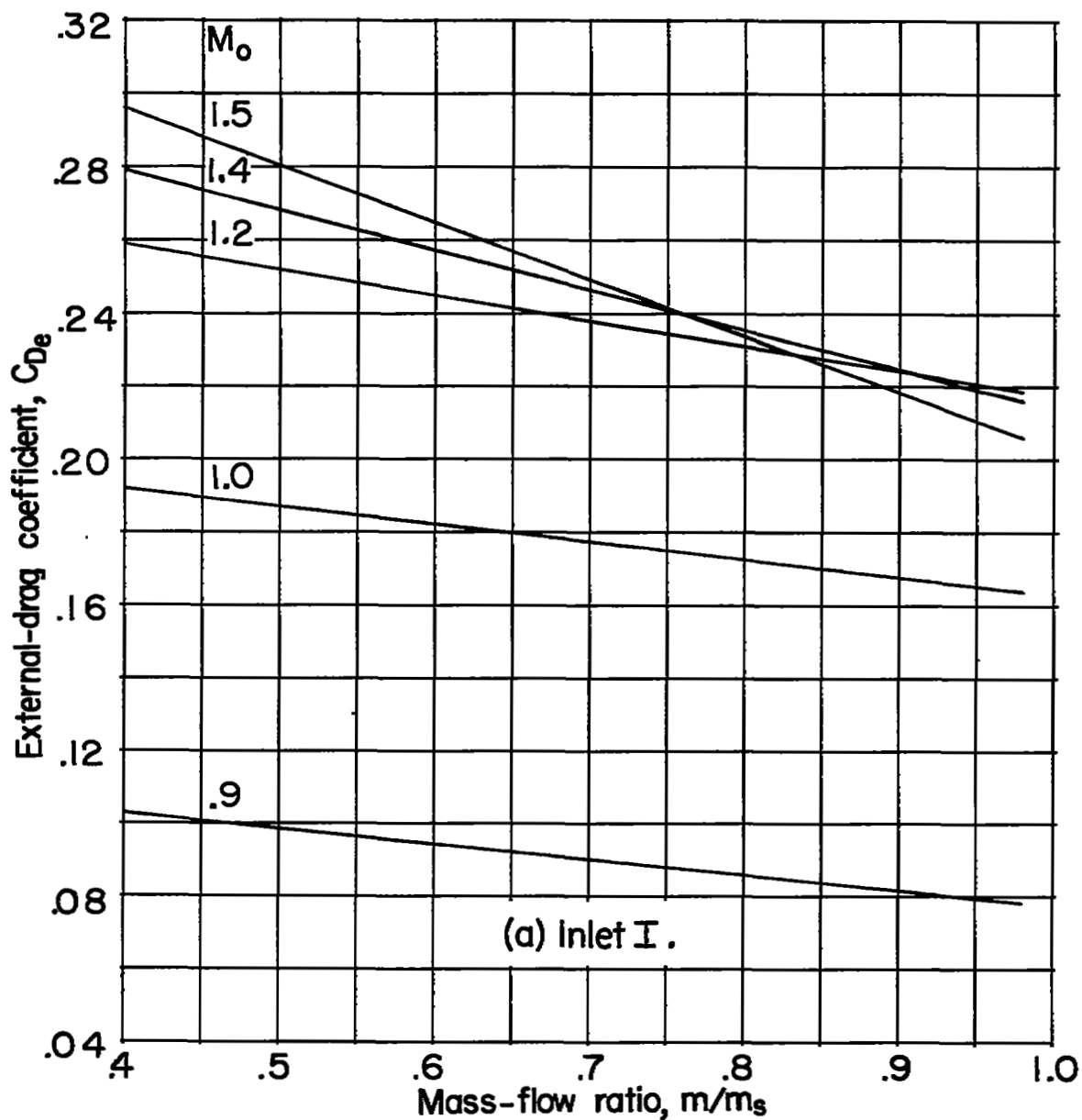


Figure 6.- Drag characteristics assumed for the nose inlets.



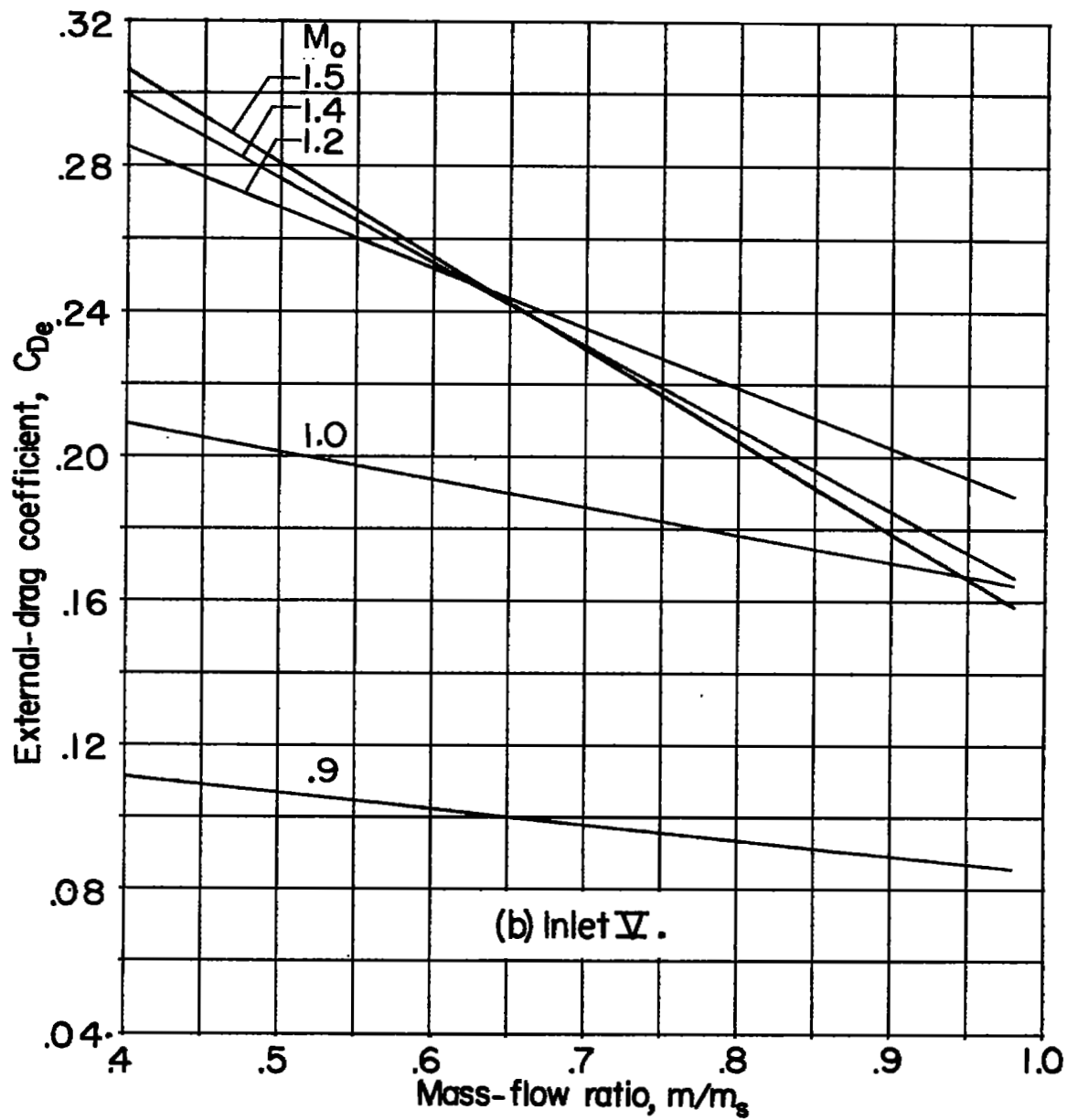


Figure 6.- Concluded.

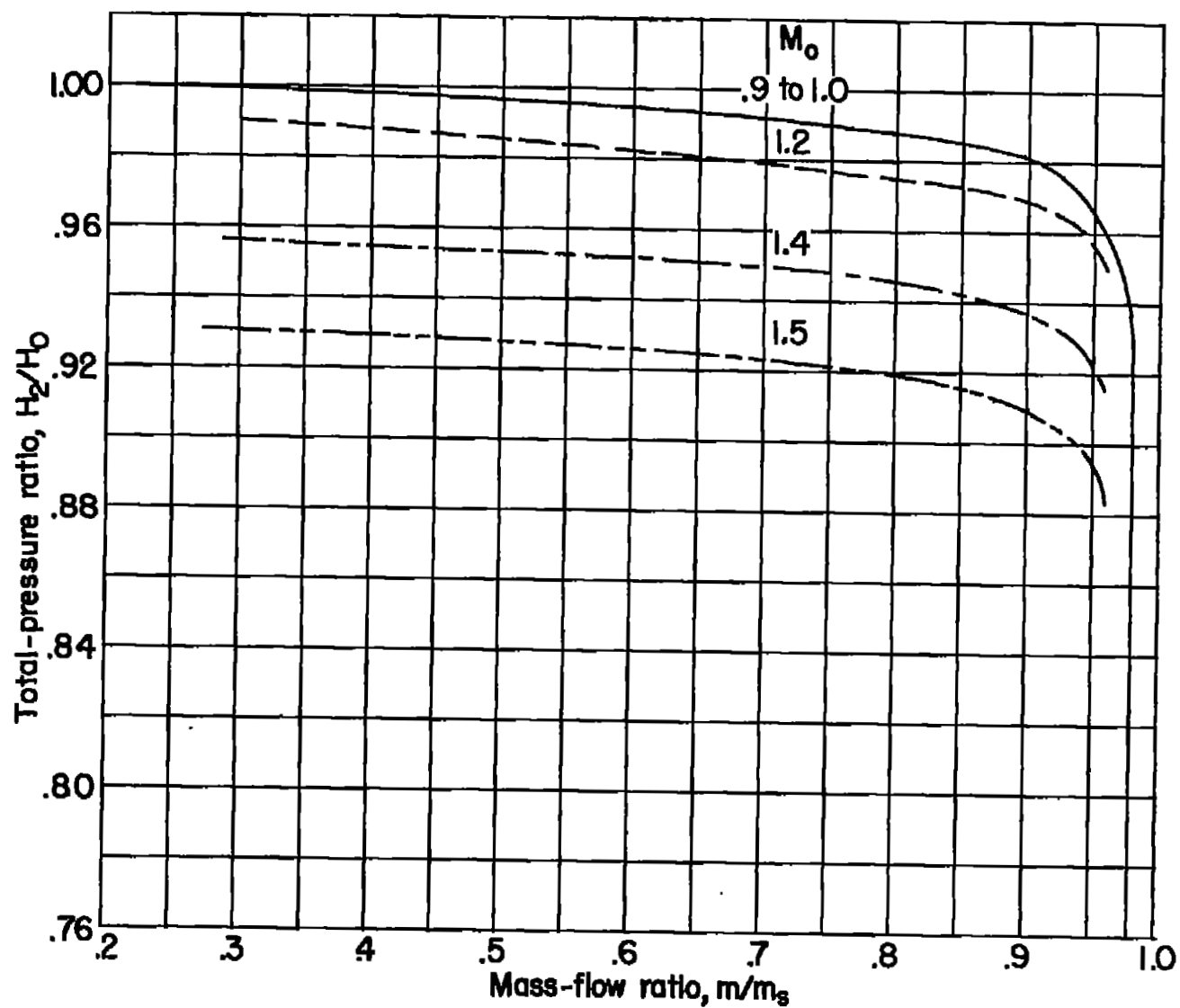


Figure 7.- Pressure-recovery characteristics assumed for nose inlets.

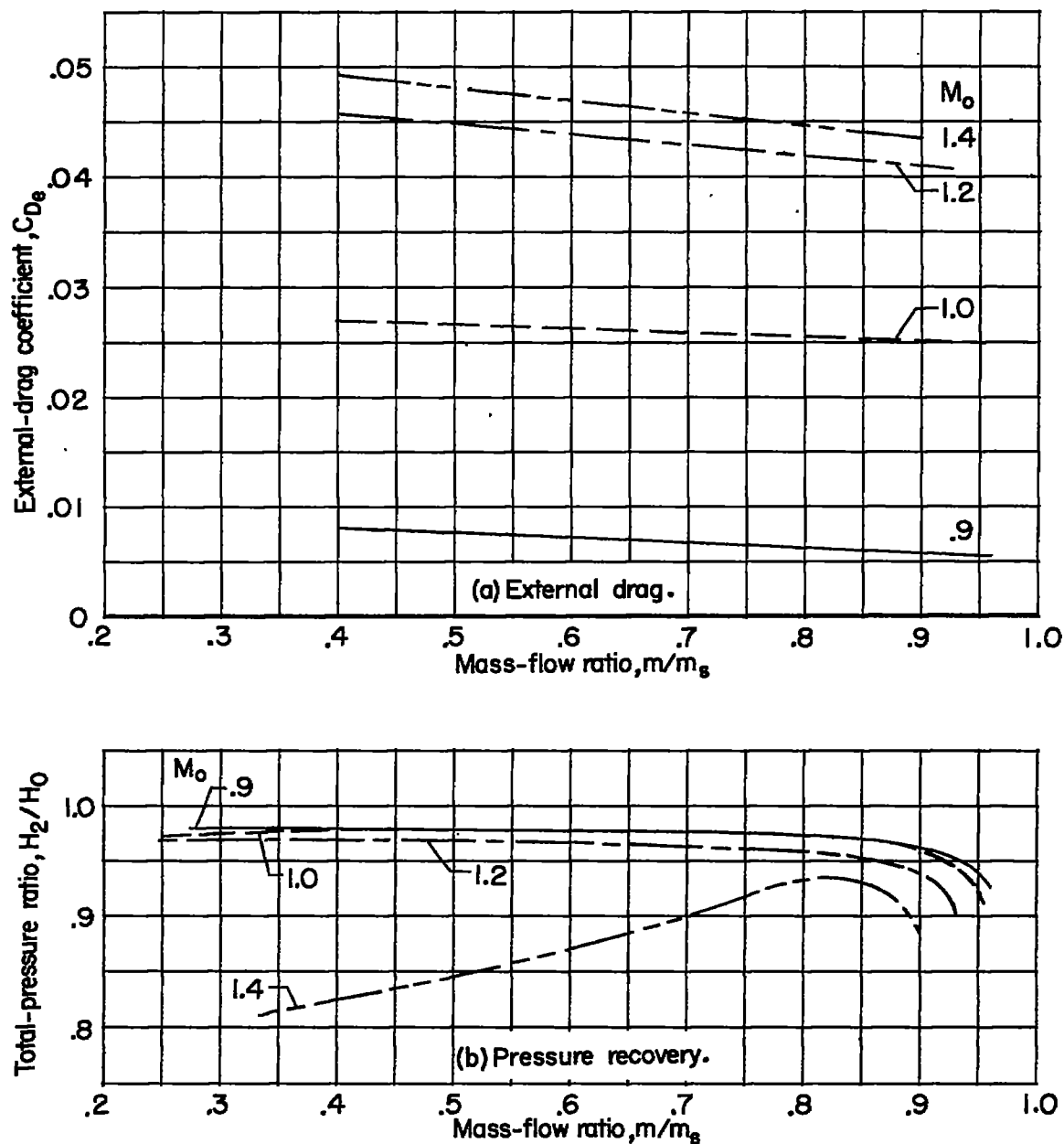


Figure 8.- Drag and pressure-recovery characteristics assumed for wing-root inlet.

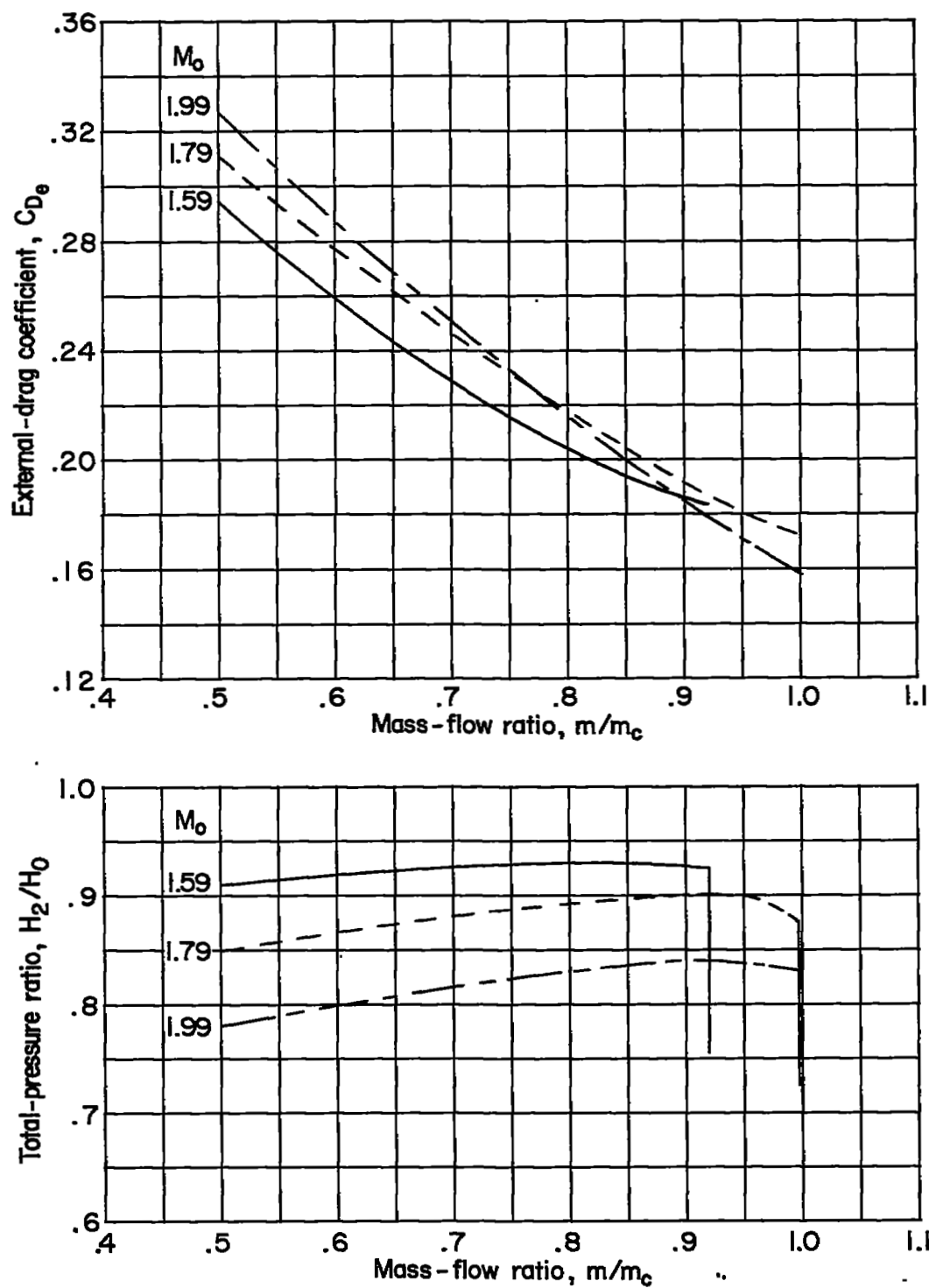


Figure 9.- Drag and pressure-recovery characteristics assumed for conical-shock inlet.

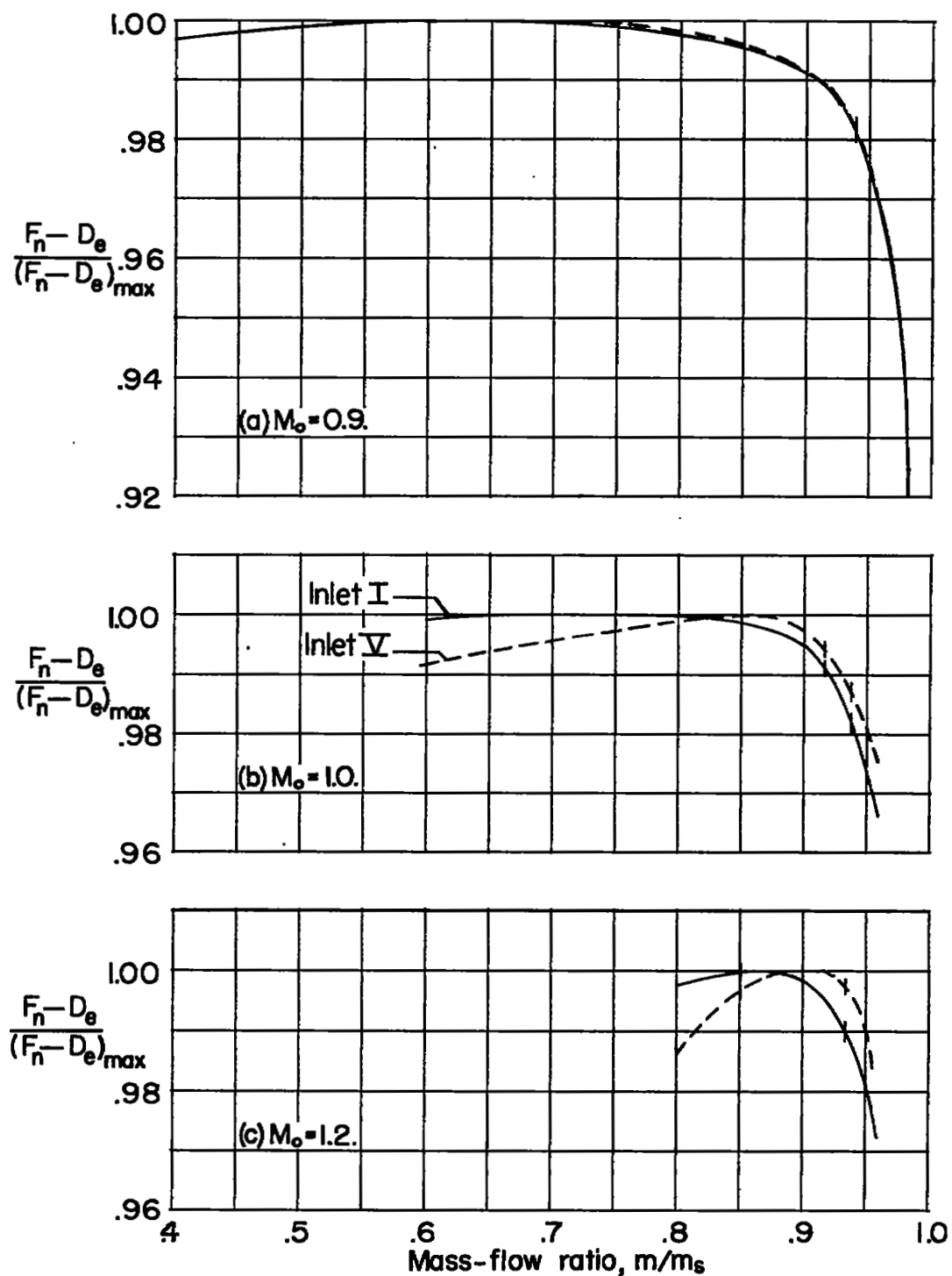


Figure 10.- Effect of mass-flow ratio on the performance of two fixed-geometry inlets.  $h = 35,000$  feet.

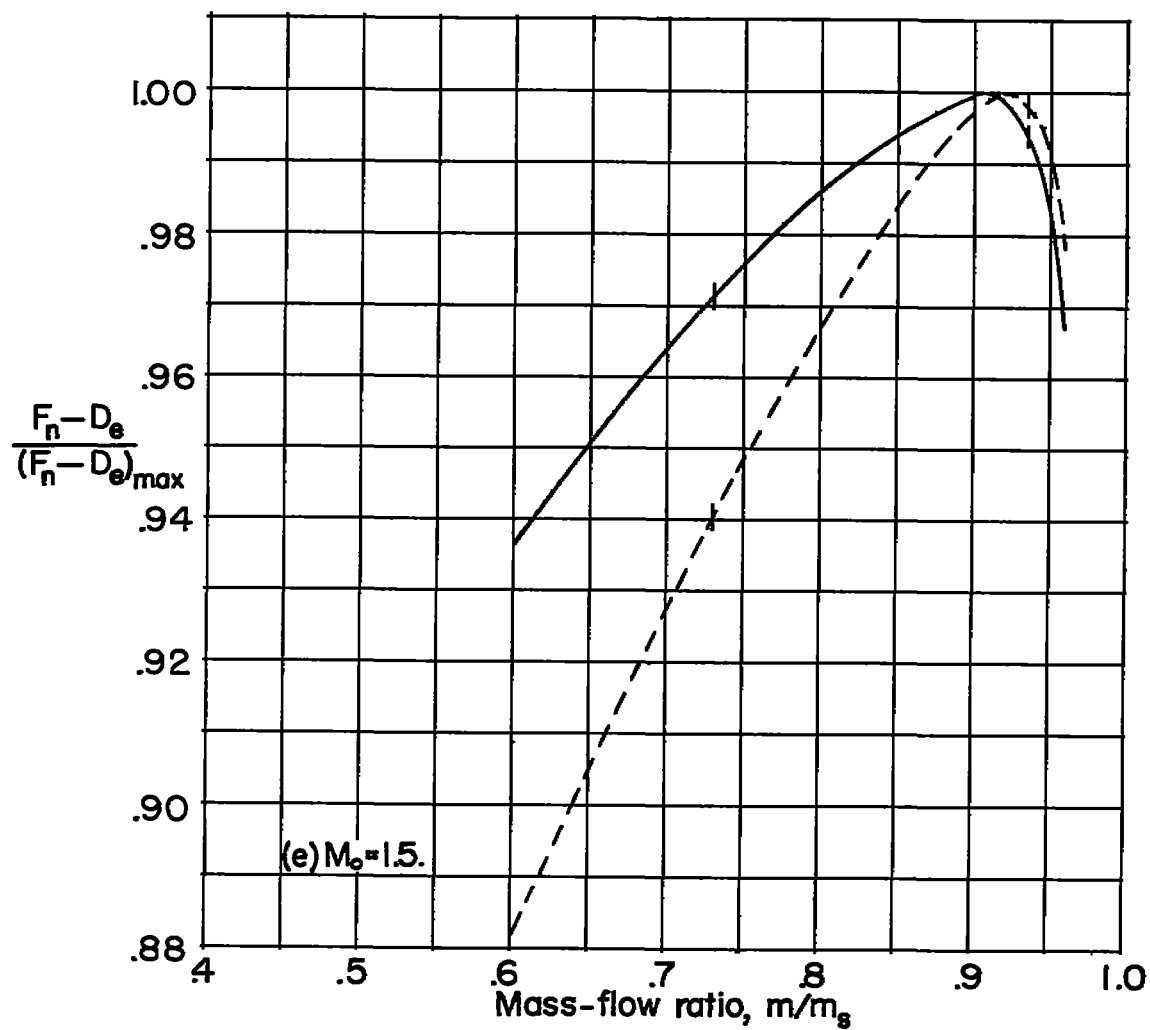
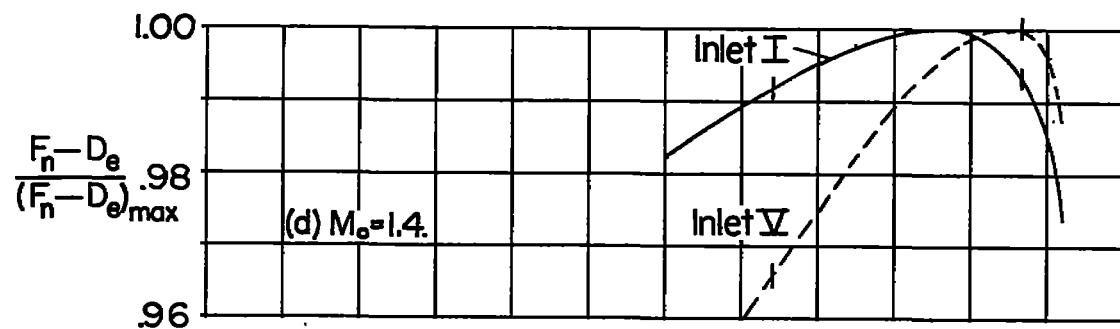


Figure 10.- Concluded.

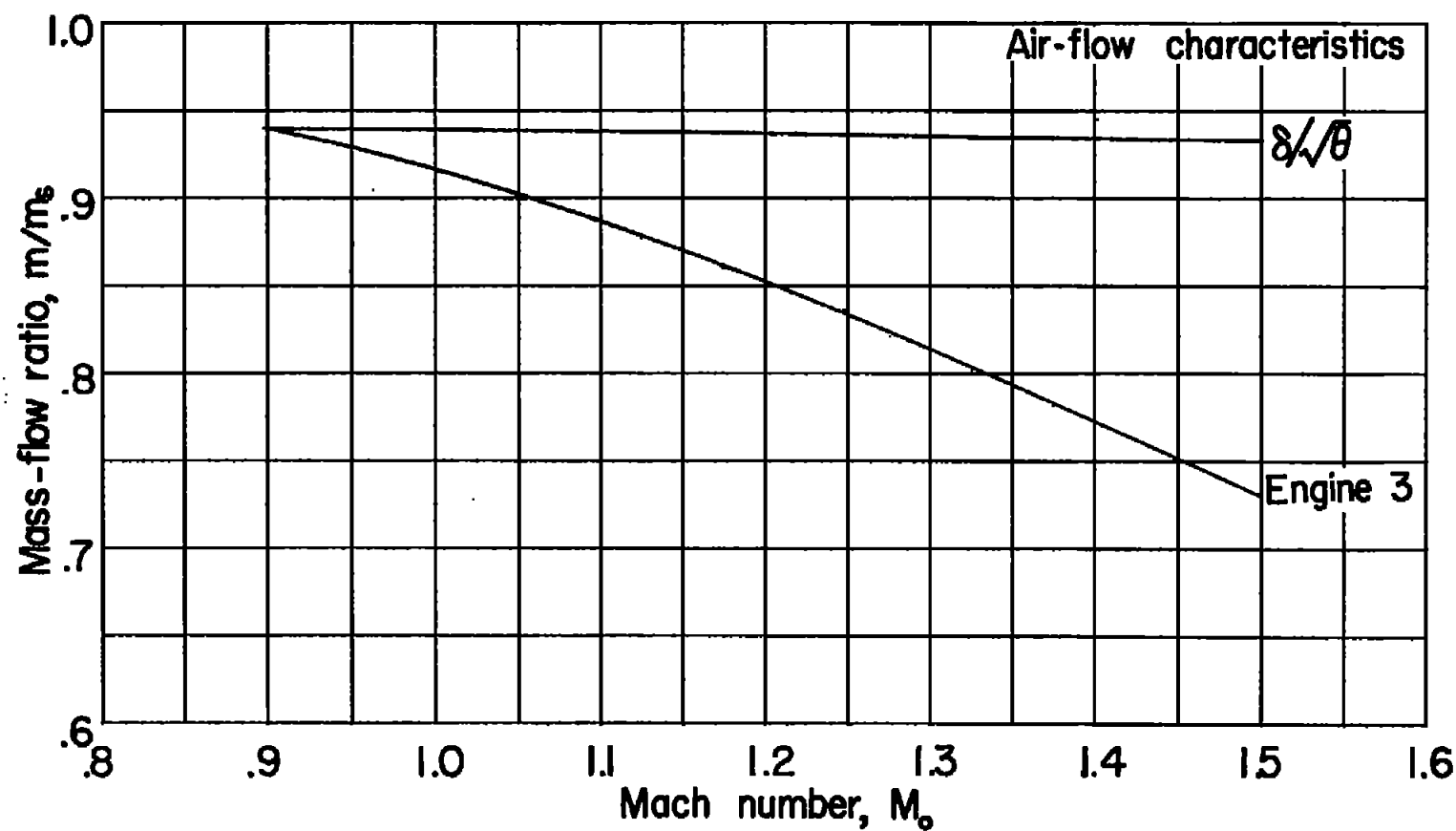


Figure 11.- Effect of engine air-flow characteristics on mass-flow-ratio requirement. Inlets I and V.

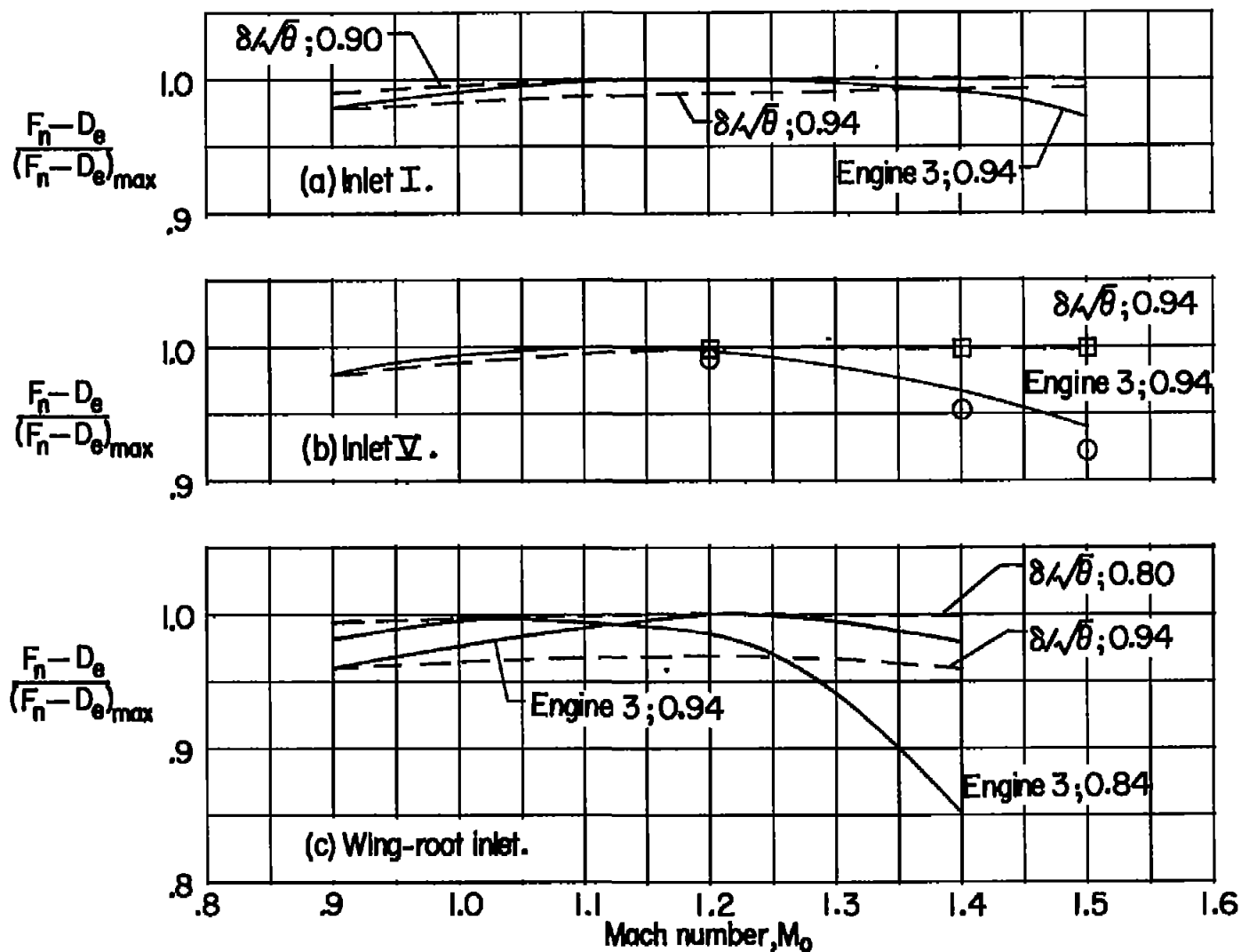


Figure 12.- Performance of several fixed-geometry systems.  $h = 35,000$  feet.  
Curves identified by engine air-flow type and design-mass-flow ratio.



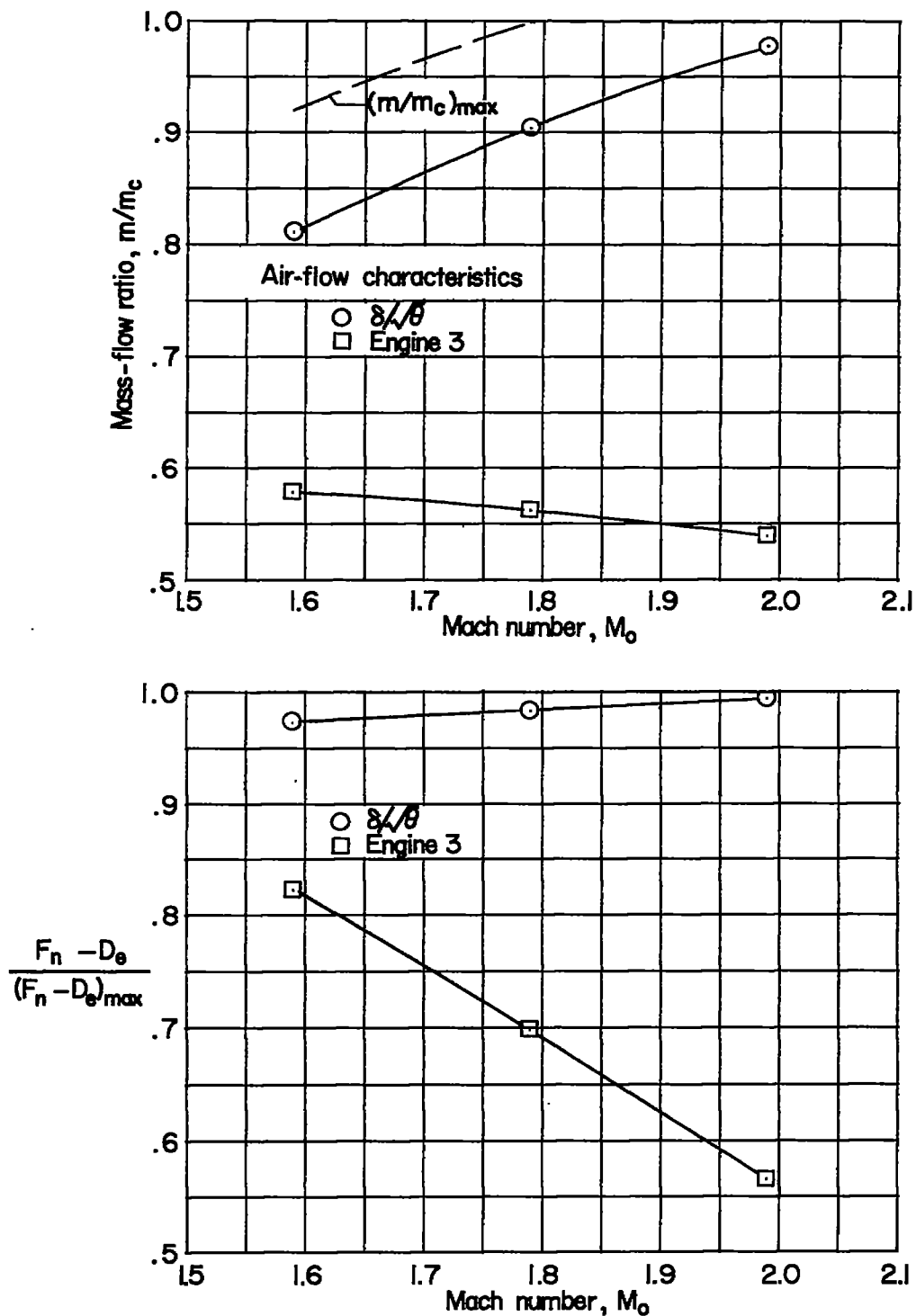


Figure 13.- Performance of a fixed-geometry conical-shock inlet matched with two different engines.  $h = 35,000$  feet.

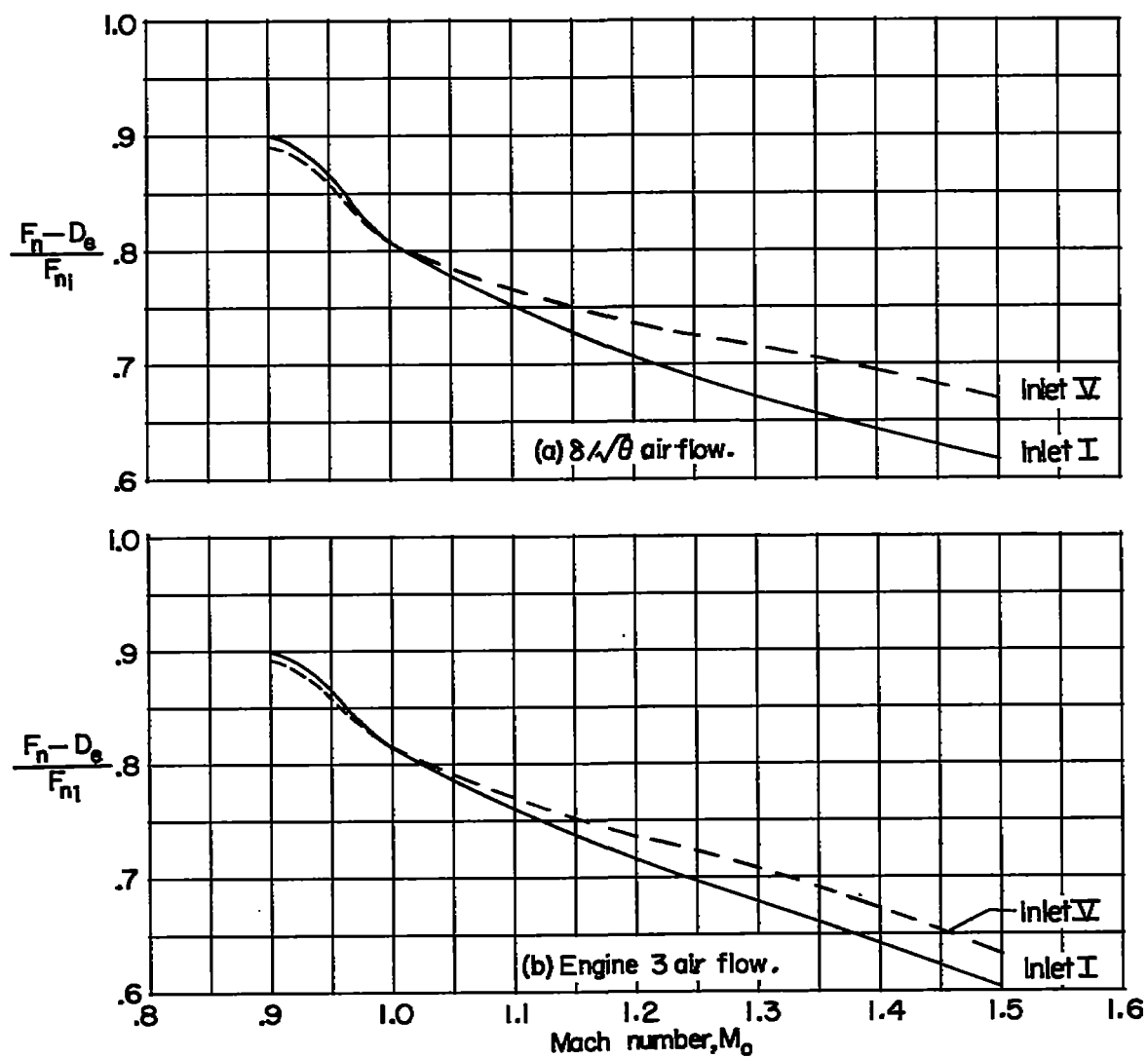


Figure 14.- Effect of inlet drag on propulsive output of four fixed-geometry systems.  $h = 35,000$  feet.

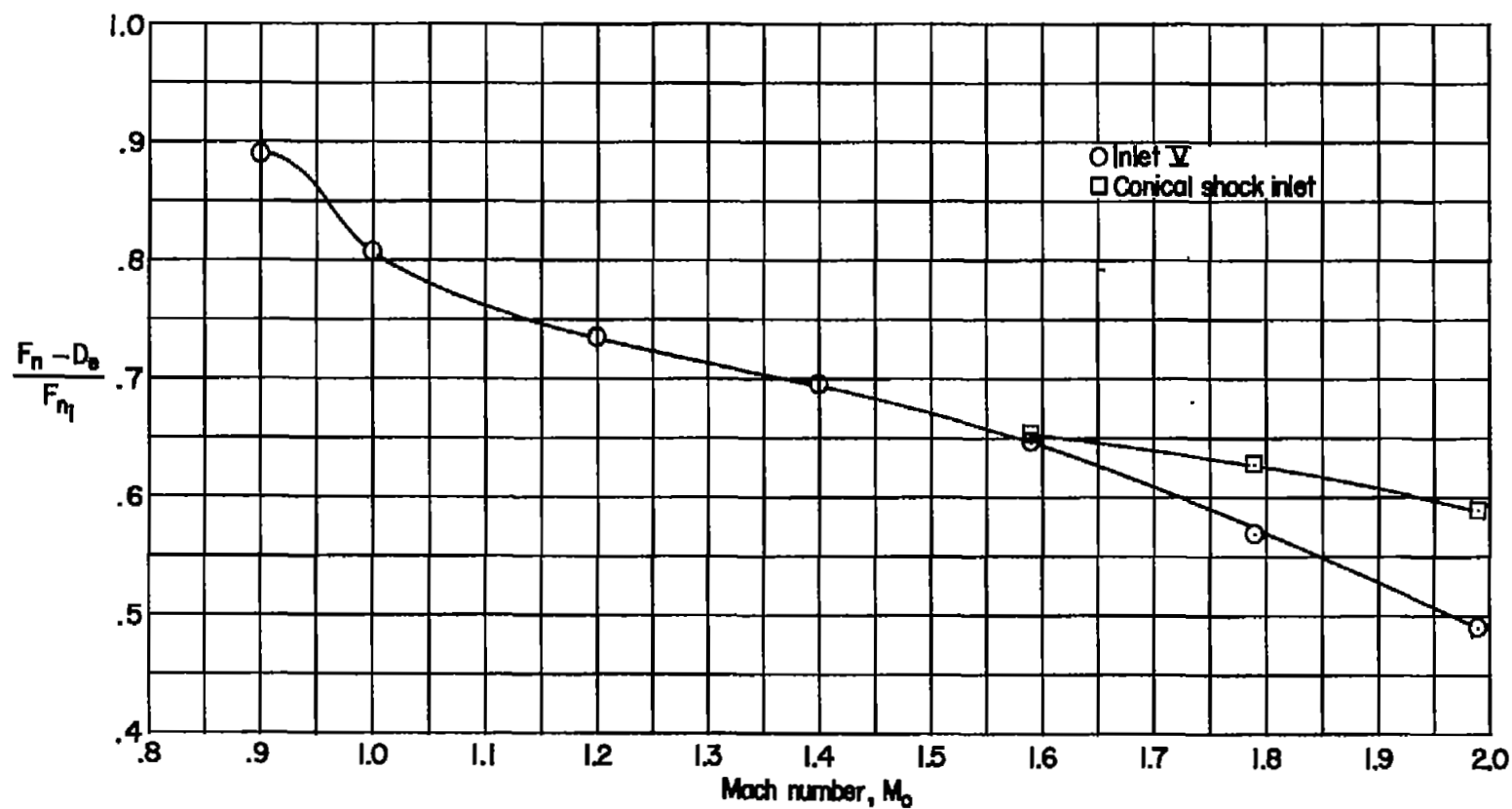


Figure 15.- Performance improvement of supersonic compression by 25° half-angle cone. Engine  $\delta/\delta$ ; fixed inlet areas;  $h = 35,000$  feet.

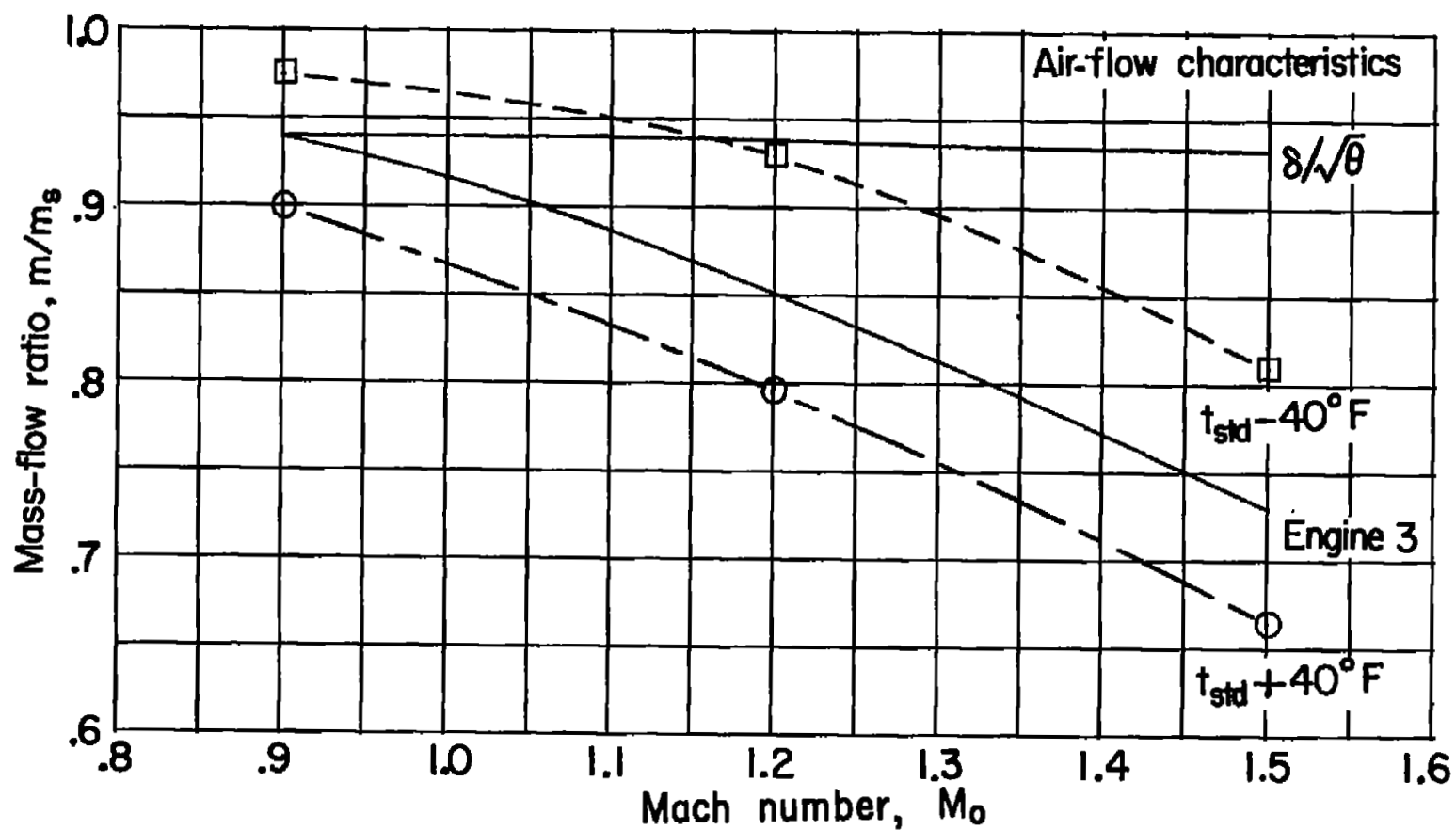


Figure 16.- Effect of temperature deviation on operating mass-flow ratios.

UNCLASSIFIED

NACA RM L54129

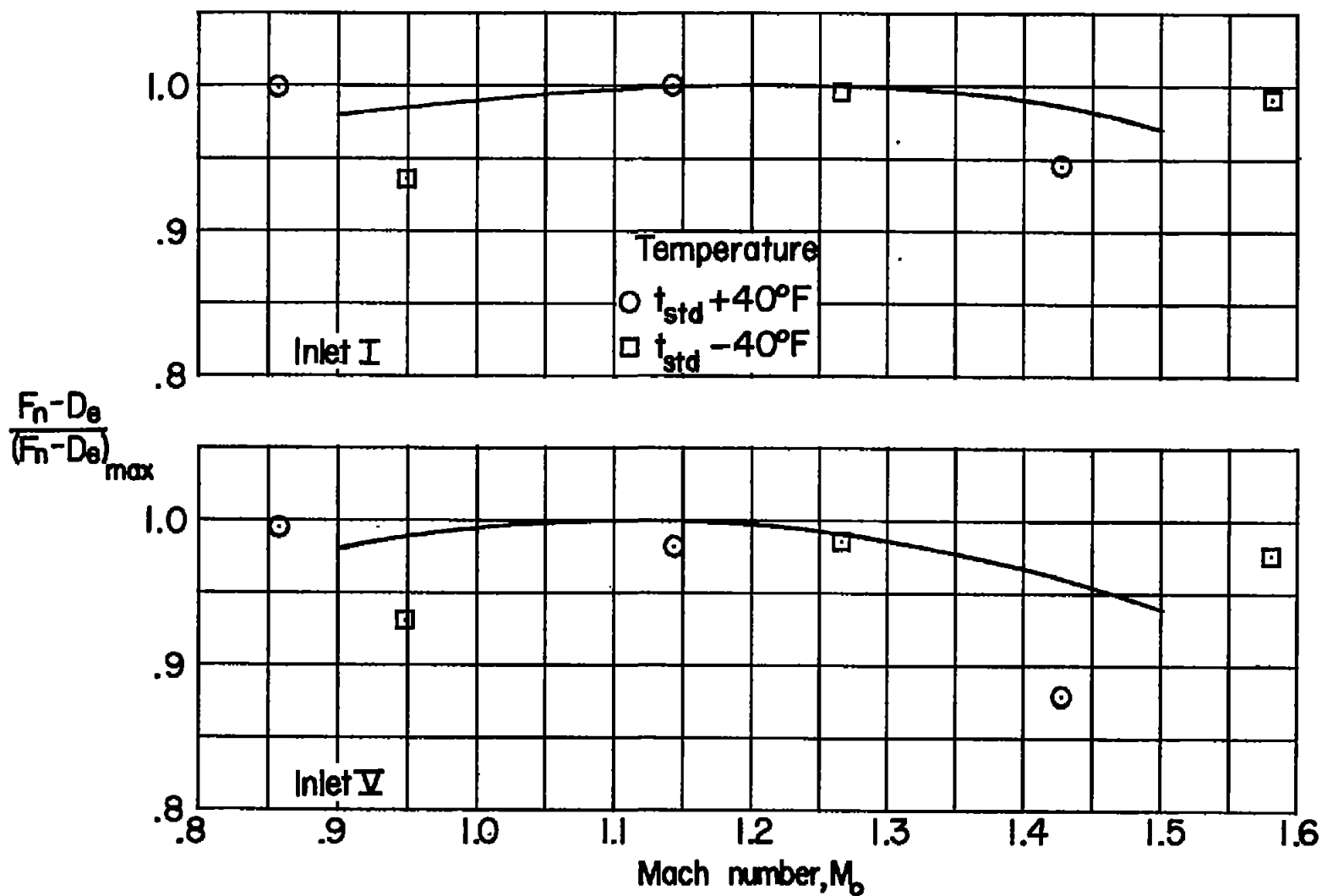


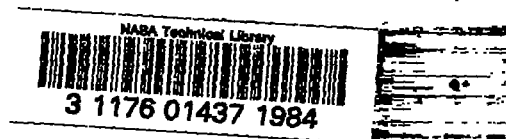
Figure 17.- Effect of temperature deviation on performance with engine 3.  
 $h = 35,000$  feet.

UNCLASSIFIED

NACA Langley - 3-4-48 - 950

UNCLASSIFIED

~~CONFIDENTIAL~~



~~CONFIDENTIAL~~

UNCLASSIFIED